

Whispering Gallery Mode Emission of a Cylindrical Droplet Laser

Mitsunori Saito and Takuya Hashimoto

Department of Electronics and Informatics, Ryukoku University, Seta, Otsu 520-2194, Japan

Keywords: Droplet Laser, Stimulated Emission, Whispering Gallery Mode, Fluorescence, Silicone Rubber.

Abstract: A cylindrical droplet laser was fabricated in a silicone rubber by using a polyethylene-glycol solution of rhodamine 6G. The silicone rubber provided a simple molding process for enclosing the droplet, since silicone oil solidified at room temperature by only adding a curing agent. Polyethylene glycol dissolved a large amount of dye molecules, yielding a fluorescent solution whose refractive index (1.46) was higher than that of the silicone rubber (1.40). Consequently, some fluorescence rays circulated in the cylindrical droplet owing to the total internal reflection on the side surface (the whispering gallery mode). Other fluorescence rays made round trips in the radial or axial directions of the cylindrical droplet (the radial and axial modes) being reflected at the side or bottom surfaces. When the droplet was excited by a green laser pulse (wavelength: 527 nm, pulse duration: 10 ns), these emission modes competed with one another to induce a stimulated emission. In a droplet with 2.0 mm diameter and 1.4 mm height, the whispering gallery mode conquered the other emission modes, exhibiting a non-linear peak growth and a peak-width narrowing when the excitation energy exceeded 20 μJ (the threshold energy of the stimulated emission).

1 INTRODUCTION

Whereas most optical devices are composed of solids, liquids exhibit some excellent functions that are unachievable with solids. Deformability (fluidity) is an attractive property when creating tunable or flexible devices. A simple fabrication process is also an advantage of liquid devices; e.g., no polishing process is needed to create a droplet with a smooth surface that acts as a microresonator (Matsko, 2009). In a smooth droplet, which is producible by spraying aerosol (Tzeng et al, 1984), lightwave circulates with a low scattering loss and generates a whispering gallery (WG) mode (Campillo et al, 1991). In addition to fundamental researches (Biswas et al, 1989), the WG mode resonators have been studied extensively in various technical fields including spectroscopy (Sasaki et al, 1997), biomedical sensing (Arnold et al, 2003), and photonic signal control (Hara et al, 2005). Of various applications, droplet lasers have been studied most keenly in the last two decades (Barnes et al, 1993). Droplets are usually suspended in air (Kaqradağ et al, 2013) or oil (Tanyeri et al, 2007), and hence, handling difficulty and instability become problems when creating a microlaser. These problems are solved by enclosing a droplet in a transparent silicone rubber (Saito et al, 2008). Although droplets in the rubber can be handled like

a solid, their deformability (optical tunability) is preserved owing to the flexibility of the rubber (Saito and Koyama, 2012). Electrical tuning is also achievable for a liquid-crystal droplet in a silicone rubber (Humar et al, 2009).

In spherical resonators the WG modes are excited in various planes because of the three-dimensional symmetry. Fluorescent microspheres, therefore, emit strong beams in various directions even in the stimulated emission process. Although the direction of the stimulated emission is controllable by deforming the sphere (Schwefel et al, 2004), creation of a cylindrical or disklike droplet is more preferable for restricting the WG mode plane. A novel fabrication process has to be developed for creation of cylindrical droplets. In addition, fabricated droplets have to be enclosed in a solid matrix, since the surface tension causes the cylinder to deform into a sphere in free space (air or oil). Silicone rubber seems useful for both creating and enclosing a cylindrical droplet.

Figure 1(a) shows the WG mode in a cylindrical droplet. Figs. 1(b) and 1(c) show two other modes in which lightwave propagates in the radial or axial direction. These modes compete with one another to induce a stimulated emission; i.e., when a stimulated emission takes place in a certain mode, it suppresses spontaneous emission of the other modes. (Saito and Ishiguro, 2006). The WG mode emission is unique

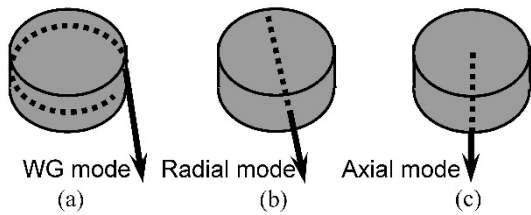


Figure 1: Schematic illustration of the emission modes in a cylindrical droplet, i.e., (a) the whispering gallery, (b) radial, and (c) axial modes.

to circulation-type resonators, whereas the other emission modes are attainable with ordinary straight waveguides. In addition, the WG mode exhibits some attractive features for uses in sensors and communications, e.g., a strong coupling with a surrounding field or neighboring resonators. It is preferred from this viewpoint to promote the stimulated emission in the WG mode. The stimulated emission occurs in a mode that has a higher gain and/or a lower loss than the other modes. The roughness of the cylinder surface causes a serious optical loss to the WG mode in comparison with the other modes, since circulating light suffers scattering at every reflection occasion. A large gain, which is related to the dye concentration and the droplet size, promotes a stimulated emission in the radial or axial mode, since lightwave is amplified strongly in a round trip between the opposing surfaces. These conditions have to be examined carefully to promote the WG mode emission.

In this study, we fabricated cylindrical droplets in a silicone rubber by using a molding technique. Then we measured fluorescence spectra by exciting a cylindrical droplet from either the flat bottom or the curved side. Spectral measurements were conducted at various positions of the droplet to evaluate the emission intensity of the three modes.

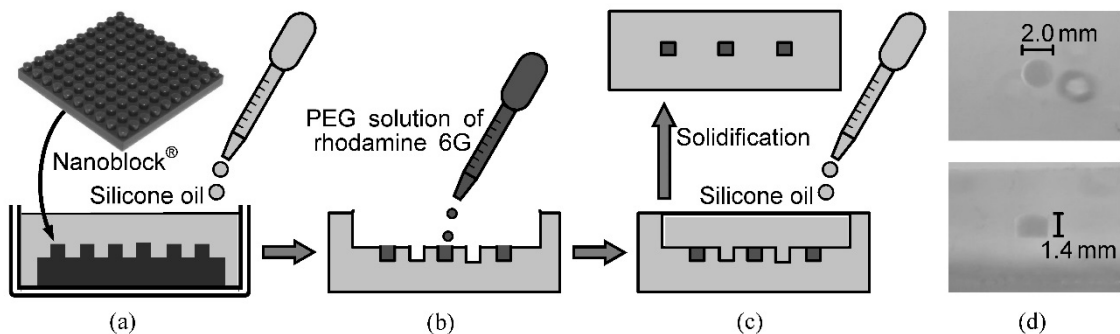


Figure 2: Fabrication process of cylindrical droplets. (a) A plastic plate with cylindrical bumps (Nanoblock®) is fixed on the bottom of a plastic case, and silicone oil with a curing agent is poured until it fills the entire case. (b) After solidification (8 h), the silicone rubber is taken out of the case. Then a dye solution is put into some selected pits that have been created by the bumps. (c) The silicone oil with the curing agent is poured into the hollow of the rubber surface to enclose the dye solution. (d) Top and side views of a droplet in the silicone rubber.

2 SAMPLE PREPARATION

Figure 2 shows the fabrication process of the cylindrical droplets. A piece of building blocks, i.e., Nanoblock® (Kawada Co., Ltd., 2012), which had bumps with 2.0 mm diameter and 1.4 mm height, was used as a mold for creating cylindrical pits on a silicone surface. As Fig. 2(a) shows, this plastic plate was placed on the bottom of a plastic case (30 mm square), and then, the case was filled up with silicone oil containing a curing agent (Shin-Etsu, KE103). The curing agent promoted a bridging reaction between silicone (polydimethylsiloxane) molecules, and consequently, the oil solidified in 8 h. As Fig. 2(b) shows, the silicone rubber that was taken out of the case had a pit array corresponding to the bumps of the plate.

A solvent for preparing a dye solution has to be selected carefully. A solvent consisting of a large molecule is preferred, since molecules of ordinary solvents, e.g., methanol and toluene, disperse into the silicone rubber through a large free volume in the flexible matrix (Saito et al, 2015). A high index of refraction is another requirement for the solvent, since the total internal reflection at the droplet surface is essential to generate the WG mode. The solubility of dye molecules is of course an important issue. Taking into account these requirements for the solvent, we selected polyethylene glycol (PEG) with a molecular weight of 300. This solvent has a refractive index of 1.46, which is higher than that of the silicone rubber (1.40). Rhodamine 6G (Tokyo Chemical Industry) was dissolved into PEG at a concentration of 10^{-3} mol/l. As Fig. 2(b) shows, this dye solution was put into some selected pits on the silicone rubber. The other pits were left empty to avoid optical interaction between neighboring droplets.

Finally, silicone oil with the curing agent was poured on the concave of the silicone rubber, as shown in Fig. 2(c). When solidification was complete (8 h later), a silicone rubber containing cylindrical droplets was obtained. The micrographs in Fig. 2(d) show the top and side views of a cylindrical droplet that is enclosed in the silicone rubber.

3 EXPERIMENT

Fluorescence spectra of the droplets were measured by using an optical system shown in Fig. 3(a). The pump light was a frequency-doubled Nd:YLF laser of 527 nm wavelength. A single pulse of 10 ns duration was shot at the occasion of a trigger signal input. The pulse energy was adjusted between 15 and 170 μJ by using an attenuator. The laser beam diameter was ~ 4 mm, and hence, the beam irradiated the entire droplet with a nearly uniform intensity distribution. Fluorescence was collected by a lens system consisting of two convex lenses and a long-pass filter that cut off the pump light. The collected light was transmitted through an optical fiber (core diameter: 400 μm) and detected by a multichannel spectrometer. Measurements were conducted in either the forward or side direction, and the detection point was changed by moving a micropositioner on which the lens system and the fiber were mounted. When the fluorescence was picked up at the cylinder edge, the WG mode emission was detected. The radial mode emission was measured by moving the pickup point to the cylinder center. The radial mode emission was measurable from the cylinder top or bottom (flat surface). As Fig. 3(b) shows, measurements were also conducted by irradiating the pump light from the cylinder top.

4 RESULTS

First, fluorescence was measured by irradiating the pump beam from the cylinder top, as shown in Fig. 3(b). Figures 4(a) and 4(b) show fluorescence spectra that were measured at the edge or the center of the curved surface, corresponding to the WG and radial modes, respectively. Figure 4(c) shows a spectrum of the axial-mode emission that emerged from the cylinder bottom (the flat surface). The radial- and axial-mode emissions exhibit a similar broad spectrum, which usually appears in a spontaneous emission process. In comparison with these spectra, the fluorescence peak of the WG-mode emission is higher and narrower. This fact indicates that the stimulated emission takes place in the WG mode. The stimulated emission, however, seems to be in its early stage, since the peak narrowing is still insufficient (FWHM: ~ 20 nm).

Next, the pump light was irradiated on the side surface of the cylinder, as shown in Fig. 3(a). Fluorescence was measured in the forward direction. Figures 5(a)–5(e) show the fluorescence spectra that were measured at several different positions by moving the pickup lens system laterally. The position that is designated as 0.0 mm corresponds to the cylinder center (the radial mode), and ± 1.0 mm corresponds to the edge (the WG mode). The pump light energy was varied between 15 and 170 μJ . As Figs. 5(d) and 5(e) show, a fluorescence peak grew nonlinearly as the pump energy increased. The peak width (FWHM) decreased to ~ 4 nm at 170 μJ . These facts indicated that a stimulated emission took place in the WG mode. The ‘red-shift’ of the fluorescence peak, which commonly takes place in the stimulated emission process of dye lasers, is also visible in the spectrum (the peak shift to 590 nm at 170 μJ). By contrast, a weak, broad fluorescence peak appeared

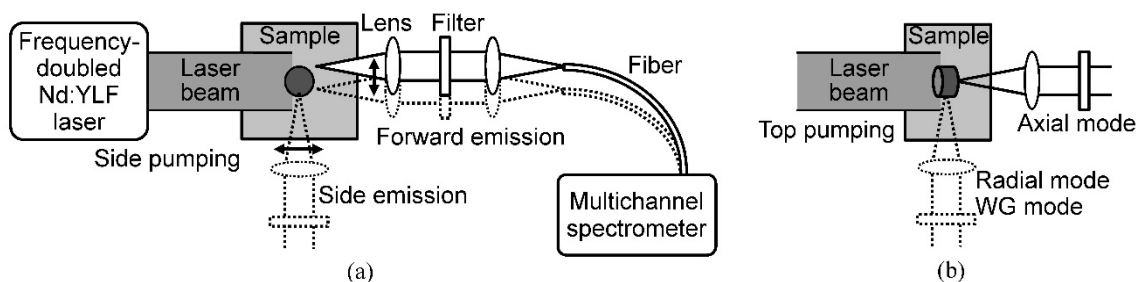


Figure 3: Optical setup for fluorescence measurements. A pump laser beam (4 mm diameter) irradiated a droplet (2 mm diameter, 1.4 mm height) from (a) the side (curved surface) or (b) the top (flat surface). Fluorescence was picked up by using a confocal lens system and a glass fiber (core diameter: 400 μm), and measured by a multichannel spectrometer. A color filter was inserted to attenuate the residual pump laser beam. As the arrows show, this pickup system was moved laterally to measure the fluorescence at the center or the edge of the droplet. Measurements were conducted in both forward and side directions.

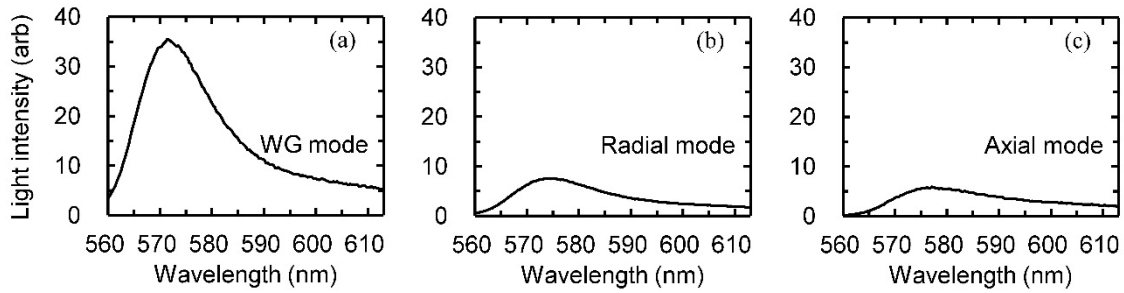


Figure 4: Fluorescence spectra that were measured by the top pumping configuration (Fig. 3(b)). (a) The WG- or (b) radial-mode emission was measured from the droplet side by adjusting the pickup position to the edge or the center, respectively. (c) The axial-mode emission was measured in the forward direction. The pulse energy and duration of the pump laser were 170 μJ and 10 ns, respectively.

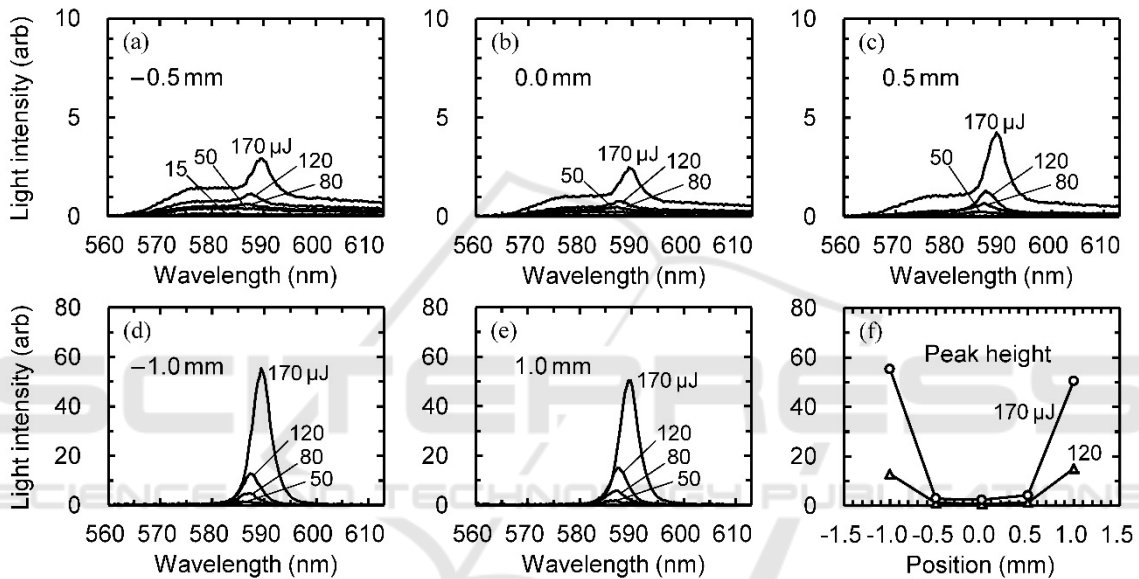


Figure 5: (a–e) Fluorescence spectra that were measured in the forward direction during the side pumping process (Fig. 3(a)). Measurements were conducted at (b) the droplet center (0.0 mm), (d, e) the edges (± 1.0 mm), and (a, c) the halfway points (± 0.5 mm). The numerals beside the spectra denote the pump energies. (f) The position dependence of the peak height.

in the other positions (0 and ± 0.5 mm), as shown in Figs. 5(a)–5(c). The peak that emerged unnaturally at 590 nm seemed to be caused by scattering of the WG-mode emission, since both the spectral shape and the pump-energy dependence of this peak resembled those in Figs. 5(d) and 5(e). Figure 5(f) shows the position dependence of the spectral peak height. The fluorescence intensities at the central portions (the radial mode) were negligible in comparison with those at the edges (the WG mode). The fluorescence in the axial direction was even weaker (below the detection limit). As these facts indicated, only a spontaneous emission took place in the radial and axial modes.

As the dotted lines in Fig. 3(a) illustrate, fluorescence measurements were conducted in the

side direction as well. Figures 6(a)–6(e) show the fluorescence spectra that were measured at various positions on the cylinder side. As Fig. 6(e) shows, a narrow peak is visible at the edge (1.0 mm) that is distant from the position of the pump light irradiation (-1.0 mm). The peak height and width are close to those measured in the forward direction (Figs. 5(d) and 5(e)). This is a reasonable result, since the WG mode usually yields the same emission intensity in all directions along the curved cylinder surface. As Fig. 6(d) shows, however, strong peaks emerged at the irradiated edge. The peak height is three-fold higher than those measured at the other edges. As Figs. 6(a)–6(c) show, the fluorescence spectra at the central portions (0 and ± 0.5 mm) are also different from those measured in

the forward direction (Figs. 5(a)–5(c)). The peak at 590 nm is thought to be caused by the scattered WG-mode light. If this peak is excluded, the radial-mode emission is weaker in the side direction than the forward direction. These phenomena are discussed in the following section. Figure 6(f) shows the peak heights that were measured at various positions. The fluorescence emission is localized at the cylinder edges, indicating occurrence of a strong WG-mode emission.

5 DISCUSSION

Let us consider the mode competition on the basis of the experimental results. The absorbance of the pump light is higher than 90% in the current droplet. This fact indicates that the dye molecules are excited more strongly on the irradiation side than the opposite side. When the pump light is irradiated from the top (Fig. 3(b)), the excitation is comparatively uniform or axially symmetrical in the droplet, and accordingly, all modes are excited evenly. As Fig. 4 shows, therefore, this excitation method yields no absolute winner of the competition; i.e., all modes emit spontaneous emission although symptoms of stimulated emission are visible in the WG mode. By contrast, when the cylinder side is irradiated (Fig. 3(a)), the central portion of the droplet receives a small pump energy,

whereas a semi-periphery on the irradiation side absorbs a strong energy. This is the reason that the axial-mode emission is negligible when the pump light is irradiated from the side. It follows that the side pumping is more preferable than the top pumping for promotion of the WG-mode emission.

The radial emission at the droplet center (0.0 mm) is stronger in the forward direction (Fig. 5(b)) than the side direction (Fig. 6(b)). This phenomenon is also explained by the non-uniformity of excitation. The radial-mode light that emerges in the forward direction passes through the irradiation point where strong excitation takes place. The radial-mode light in the side direction, however, passes the region apart from the excitation point. This difference in the excitation strength causes the anisotropy in the radial-mode emission.

As mentioned earlier, the WG mode usually emits fluorescence uniformly along its optical path (the periphery). If a portion of the optical path is excited strongly, however, the circulating light is amplified strongly at that portion. Since the outward radiation is proportional to the circulating light intensity, the WG-mode emission possibly becomes strong at around the excitation point. This is the reason that the strong fluorescence peak emerges at the irradiation edge (Fig. 6(d)). This local radiation enhancement seems useful to extract a light energy efficiently at a specific point. If the circulating light is confined strongly in the droplet, i.e., if the WG

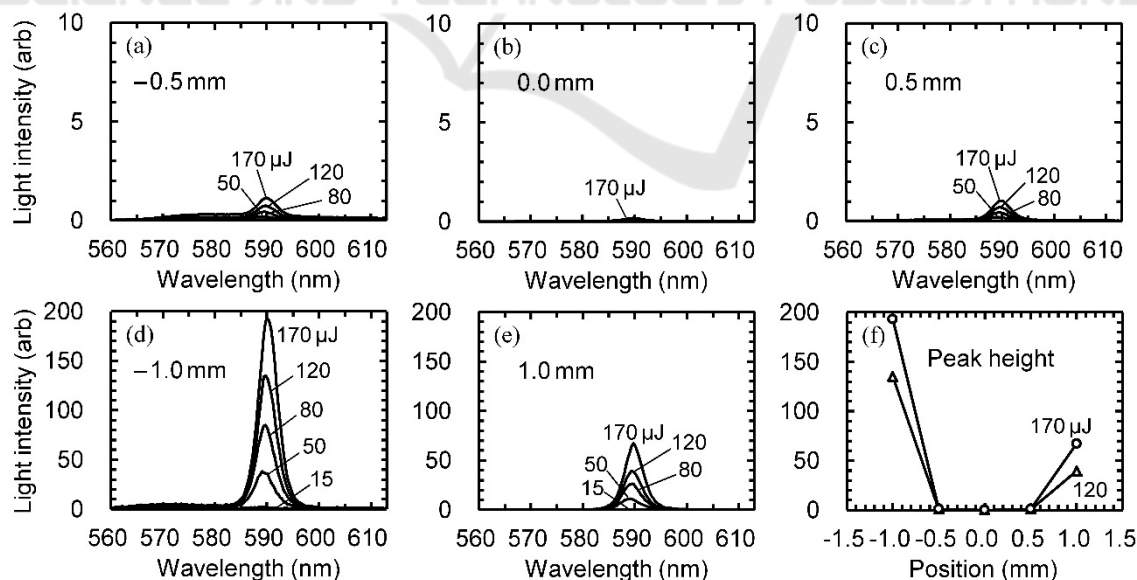


Figure 6: (a–e) Fluorescence spectra that were measured in the direction perpendicular to the pump beam axis, i.e., the downward direction in Fig. 3(a). Measurements were conducted at different positions; i.e., (b) the droplet center (0.0 mm), (d) the pumping side (–1.0 mm), (e) the opposite side (1.0 mm), and (a, c) the halfway points (± 0.5 mm). The numerals beside the spectra denote the pump energies. (f) The position dependence of the fluorescence peak height.

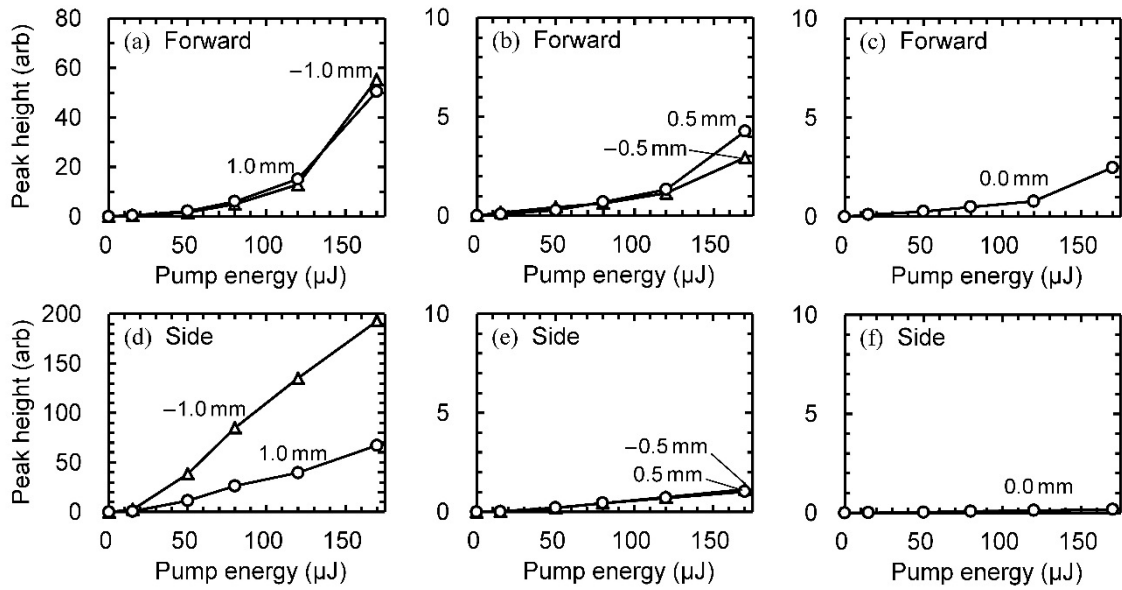


Figure 7: The pump-energy dependence of the fluorescence intensity (peak height). (a)–(c) and (d)–(f) correspond to the data that were shown in Figs. 5 and 6, respectively. (a) and (d) show the data for the WG-mode emission. (c) and (f) show the data for the radial-mode emission.

mode is weakly coupled to the outer electromagnetic field, the outward radiation loss is small, and hence, the circulating light propagates to the opposite side with a small attenuation. If this is the case, the intensity of the WG-mode emission becomes the same at all positions; i.e., no local radiation enhancement takes place. From this viewpoint, it is preferable to enclose a droplet in a silicone rubber, since a small difference in their refractive indices enhances a coupling efficiency between the WG mode and the outer field.

Figures 7(a)–7(c) show the pump-energy dependences of the fluorescence peak height, which were plotted on the basis of the experimental results in Fig. 5 (the forward direction). As Fig. 7(a) shows, the WG-mode emission exhibits a nonlinear peak growth when the pump energy exceeds 50–100 μJ . Although similar nonlinear characteristics are visible at the other positions (Figs. 7(b) and 7(c)), the spectral peaks at these positions are attributed to the scattering of the WG-mode light. Figure 7(d) shows the peak heights of the WG mode that were measured in the side direction (Figs. 6(d) and 6(e)). At the irradiated edge (–1.0 mm), the stimulated emission takes place when the pump energy exceeds ~ 20 μJ . As regards the opposite edge (1.0 mm), the threshold is not clear, i.e., the gradient of the curve increases gradually as the pump energy increases. This gradual increase is similar to those of the curves in Fig. 7(a). The plots in Figs. 7(e) and 7(f) also show a similar dependence (gradual increase)

on the pump energy. It is therefore assumed that these emission peaks are caused by scattering of the WG mode light.

In the current experiments, the silicone rubber proved to be useful for both shaping a cylindrical droplet and providing a suitable refractive index. PEG is also a promising solvent, since it induces random lasing in the translucent solid phase (Saito and Nishimura, 2016). With these useful materials, we are currently planning new experiments, which include spectral tuning by sample deformation, near-field coupling of the cylindrical droplets, and bistable laser emission owing to the phase transition in PEG.

6 CONCLUSIONS

A fabrication process of a cylindrical droplet laser was established by using a molding technique of a silicone rubber. A stimulated emission in the WG mode was realized by exciting the droplet (2.0 mm diameter and 1.4 mm height) with a green laser pulse (10 ns, 20 μJ). The excitation from the curved surface was effective for both suppression of the other emission mode and efficient extraction of the WG mode emission. The combination of silicone rubber and polyethylene glycol can be extended to creation of various composite materials and devices including a flexible microresonator and a droplet laser array.

ACKNOWLEDGEMENTS

This research was supported by Japan Society for the Promotion of Science (15K04642).

REFERENCES

- Matsko, A. B., ed., 2009. *Practical Applications of Microresonators in Optics and Photonics*, CRC Press. Boca Raton, Florida.
- Tzeng, H.-M., Wall, K. F., Long, M. B., Chang, R. K., 1984. Laser emission from individual droplets at wavelengths corresponding to morphology-dependent resonances. *Opt. Lett.* 9(11). p. 499–501.
- Campillo, A. J., Eversole, J. D., Lin, H.-B., 1991. Cavity quantum electrodynamic enhancement of stimulated emission in microdroplets. *Phys. Rev. Lett.* 67(4). p. 437–440.
- Biswas, A., Latifi, H., Armstrong, R. L., Pinnick, R. G., 1989. Time-resolved spectroscopy of laser emission from dye-doped droplets. *Opt. Lett.* 14(4). p. 214–216.
- Sasaki, K., Fujiwara, H., Masuhara, H., 1997. Optical manipulation of a lasing microparticle and its application to near-infrared microspectroscopy. *J. Vac. Sci. Technol. B*, 15(6). p. 2786–2790.
- Arnold, S., Khoshsima, M., Teraoka, I., Holler, S., Vollmer, F., 2003. Shift of whispering-gallery modes in microspheres by protein adsorption. *Opt. Lett.* 28(4). p. 272–274.
- Hara, Y., Mukaiyama, T., Takeda, K., Kuwata-Gonokami, M., 2005. Heavy photon states in photonic chains of resonantly coupled cavities with supermonodisperse microspheres. *Phys. Rev. Lett.* 94(20). p. 203905-1–4.
- Barnes, M. D., Ng, K. C., Whitten, W. B., Ramsey, J. M., 1993. Detection of single rhodamine 6G molecules in levitated microdroplets. *Anal. Chem.* 65(17). p. 2360–2365.
- Kaqradağ, Y., Aas, M., Jonáš, A., Anand, S., McGloin, D., Kiraz, A., 2013. Dye lasing in optically manipulated liquid aerosols. *Opt. Lett.* 38(10). p. 1669–1671.
- Tanyeri, M., Perron, R., Kennedy, I. M., 2007. Lasing droplets in a microfabricated channel. *Opt. Lett.* 32(17). p. 2529–2531.
- Saito, M., Shimatani, H., Naruhashi, H., 2008. Tunable whispering gallery mode emission from a microdroplet in elastomer. *Opt. Express*, 16(16). p. 11915–11919.
- Saito, M., Koyama, K., 2012. Spatial and polarization characteristics of a deformed droplet laser. *J. Opt.* 14(6). p. 065002-1–6.
- Humar, H., Ravnik, M., Pajk, S., Muševič, I., 2009. Electrically tunable liquid crystal optical microresonators. *Nature Photon.* 3. p. 595–600.
- Schwefel, H. G. L., Rex, N. B., Tureci, H. E., Chang, R. K., Stone, A. D., Ben-Messaoud, T., Zyss, J., 2004. Dramatic shape sensitivity of directional emission patterns from similarly deformed cylindrical polymer lasers. *J. Opt. Soc. Am. B*, 21(6). p. 923–934.
- Kawada Co., Ltd. (Japan), 2012. *What's Nanoblock?* <http://www.diablock.co.jp/kawada/en/nanoblock/about>.
- Saito, M., Ishiguro, H., 2006. Anisotropic fluorescence emission of a dye-doped fibre ring that is pumped by a ring laser beam. *J. Opt. A: Pure Appl. Opt.* 8(1). p. 208–213.
- Saito, M., Nishimura, T., Hamazaki, T., 2015. Fade-resistant photochromic reactions in a self-healable polymer. *Opt. Express*, 23(20). p. 25523–25531.
- Saito, M., Nishimura, Y., 2016. Bistable random laser that uses a phase transition of polyethylene glycol. *Appl. Phys. Lett.* 108(13). p. 131107-1–4.